Journal of GeoEngineering, Vol. 15, No. 1, pp. 47-54, March 2020
http://dx.doi.org/10.6310/jog.202003_15(1).4

STUDY ON SHAFT FRICTION OF OPEN-ENDED STEEL PIPE PILES FOR OFFSHORE WIND FARMS BASED ON FIELD TESTS

Zhong-Bo Hu [1*], Shen Huang [2], Wei Liu [3], and Jing Si [3]

ABSTRACT

Many offshore wind farms have already been constructed and more are planned in China. Monopiles with pile diameter more than 1.5 m are the main foundation form of wind turbine generators. The determination of the axial pile capacity (especially shaft resistance) of monopiles is one of the important issues for offshore structures. A series of full-scale offshore static load tests of open-ended steel pipe piles are conducted at two thick overburden-layer sites. The load-settlement curve at pile head, axial force and inner and outer friction-resistance ratio (friction-resistance ratio) along the pile shaft are derived. The results show that the inner shaft friction is indispensable for large-diameter open-ended steel pipe piles, and the piles are approximately full cored. At the upper 3 m close to the ground surface, the friction-resistance ratio is relatively small, and the average value is about 0.15. An increasing trend with depth is obvious. At the critical depth region, the average ratio in the cohesive soil and cohesionless soil varies from 0.28 to 0.43 and 0.26 to 0.40, respectively. Furthermore, the ratio continues to increase as it goes deeper, and the maximum ratio is no more than 0.5. A new design method considering the influence of pile diameter and embedded depth is employed to calculate the inner and outer friction-resistance ratio. The performance of the new design method is assessed against the field test results.

Key words: Offshore wind farms, open-ended steel pipe piles, shaft friction, inner and outer friction-resistance ratio, field tests.

1. INTRODUCTION

In recent years, global energy supply has continued to be tense, and countries are actively developing new energy industries. Offshore wind energy has gradually become an industry direction in the world. In order to replace fossil energy with renewable energy sources, more and more offshore wind farms are being constructed in China. As the foundations for offshore wind power plants, open-ended steel pipe piles are becoming increasingly important in constructing offshore structures. The axial capacity depends on many factors, and a plug may form during the pile installation, which may induce uncertainty in axial capacity. The uncertainty in the axial bearing capacity may be largely attributed to the complicated behavior of soil plugging (Yu *et al.* 2012).

Figure 1 shows three cases of plugging for an open-ended steel pipe pile, *i.e.,* fully plugged, partially plugged and fully coring. When the pile is fully plugged (Fig. 1(a)), the pile behaves like a close-ended pile. The axial bearing capacity consists of two components: tip resistance and shaft resistance. For the open-ended pipe pile, the tip resistance is further decomposed into annulus and plug resistance (Paikowsky and Whitman 1990). When the pile is partially plugged (Fig. 1(b)), a plug may be formed inside the pile, and there is an additional inner friction resistance being mobilized, though the plug is lower than the fully coring pile. When the pile is fully coring (Fig. 1(c)), the pile is filled with the plug, and the axial bearing capacity is achieved by an inner and outer shaft resistance and the tip resistance mobilized by pile annulus.

Currently, several improved methods have been developed to determine the axial bearing capacity, *e.g.,* Fugro-05 (Kolk *et al.* 2005), ICP-05 (Jardine *et al.* 2005), NGI-05 (Clausen *et al.* 2005), UWA-05 (Lehane *et al.* 2005), HKU-12 (Yu and Yang 2012) and the German approach proposed by Lüking and Becker (2015). Among all the approaches, only the German approach considers the impact of plug, which considers three cases as follows: (a) fully

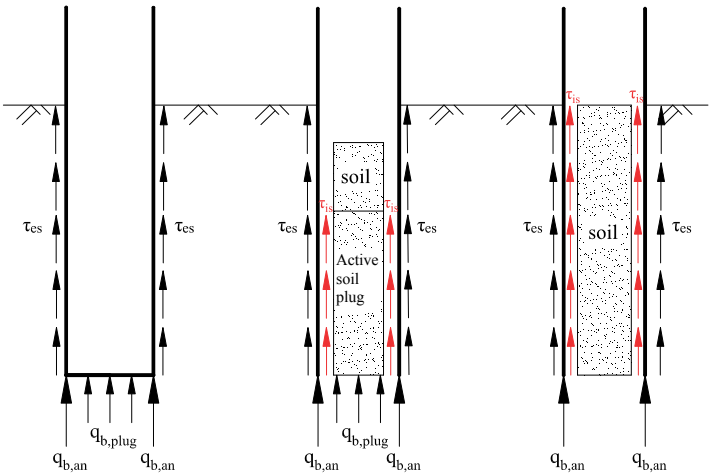

Note: $q_{b.an}$ is the annulus resistance of the open-ended pipe pile (kPa)
$q_{b.plug}$ is the plug resistance of the open-ended pipe pile (kPa)
τ_{is} is the inner shaft friction of the open-ended pipe pile (kPa)
τ_{es} is the outer shaft friction of the open-ended pipe pile (kPa)

Fig. 1 Axial bearing behavior of a open-ended pipe pile

Manuscript received April 8, 2019; revised August 8, 2019; accepted September 3, 2019.
[1*] Ph.D. (corresponding author), Senior Engineer, PowerChina Chengdu Engineering Corporation Limited, Sichuan, China (E-mail:huzhongbo87@163.com).
[2] Ph.D. Candidate, Department of Architecture and Civil Engineering, Beijing University of Technology, Beijing, China.
[3] Senior Engineer, PowerChina Chengdu Engineering Corporation Limited, Sichuan, China.

plugged with $D \le 0.5$ m; (b) fully coring with $D \ge 1.5$ m; (c) partially plugged with 0.5 m < D < 1.5 m (D is the outer pile diameter). Observations by Jardine *et al.* (2005) show that the open-ended steel pipe pile is likely to form a plug with a diameter less than 1.5 m. The diameter of steel pipe piles used in offshore wind farms is generally in the range of 6 to 10 m. This means that no plugging effect is expected and the bearing behavior exhibits fully coring. The pile bearing capacity is composed of annulus, inner and outer shaft resistance. The pile-soil interface behavior is of particular interest where shaft friction plays an important role in resisting the applied load. Among the 113 pile load tests of open-ended steel pipe piles with diameters varying from 0.32 m to 1.42 m, the German approach assumed that the inner shaft friction is not acting at the upper 20% of the embedded length of the pile, and reduced to 50% of the outer shaft friction of the rest part. More recently, several improved methods for estimation shaft friction of pipe piles have been developed to account for the influence of plugging degree (*e.g.,* Kyuho *et al.* 2003; Yu and Yang 2012). Whether the assumption of the Germany approach is applicable to large-diameter steel pipe piles ($D \ge 1.5$ m) needs to be further studied.

In this paper, 4 full-scale static load tests for large-diameter steel pipe piles were conducted at two thick overburden-layer sites. The piles were fully instrumented before driving, and tested to failure. The distribution of inner and outer shaft friction in different soil were discussed with particular attention to their contribution to the shaft resistance. An effort has been made to develop a new design method to correlate the inner shaft resistance to the axial bearing capacity. The result of this paper could serve as a guide to help engineers to advance the understanding of the axial load response behavior of an offshore foundation.

2. MAJOR DESIGN METHODS

For large-diameter steel pipe piles, the compressive bearing capacity of an axially pile consists of annulus resistance and shaft resistance. Most design methods can not differentiate shaft resistance between inner and outer shaft resistance. In practice, an additional resistance due to friction between the pile inner shaft area and the inner soil is mobilized in the unplugged case. The force equilibrium diagram of section i is shown in Fig. 2.

The pile resistance for the unplugged condition is given by Eq. 1:

$$F_i + G_i = F_{i+1} + f_{i,ins} A_{si} + f_{i,out} A_{si} \tag{1}$$

where F_i and F_{i+1} is the axial force of upper and lower section, respectively; $f_{i,ins}$ and $f_{i,out}$ is the inner and outer shaft friction of section i, respectively; G_i and A_{si} is the effective weight and pile area of section i, respectively.

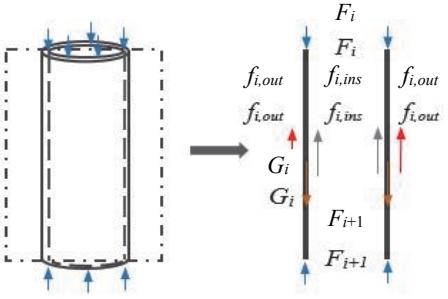

Fig. 2 Pile force equilibrium diagram

In this paper, three different analytical methods were introduced to determine the outer shaft friction of steel pipe piles. The methods are the API method (American Petroleum Institute 2010), USACE method (U.S. ACE 1990) and CPH method (Ministry of Communications of People's Republic of China 2002).

2.1 API Method

The API procedures for clay are based essentially on the use of undrained shear strength and are largely empirical. The following equation is introduced to determine outer shaft friction in cohesive soil:

$$f = \alpha\, c_u \tag{2}$$

where f is the outer shaft friction in clay; c_u is the undrained shear strength of soil; α is the coefficient that is a function of c_u:

$$\alpha = \begin{cases} 1 & , \quad \psi \le 0.25 \\ 0.5\psi^{-0.5} & , \quad 0.25 < \psi < 1 \\ 0.5\psi^{-0.25} & , \quad \psi \ge 1 \end{cases} \tag{3}$$

$\psi = c_u/P_0$, P_0 is the effective overburden pressure.

The API procedures for sand is also strongly empirical but based on effective-stress because no excess pore water pressure was assumed. Equation (4) shows the recommendations for outer shaft friction of pipe piles in cohesionless soil:

$$f = k(\tan\delta)\, P_0 \tag{4}$$

where k is the coefficient of lateral earth pressure (k = 0.8 and 1.0 was recommended for open-ended pipe piles and full displacement piles, respectively); δ is the friction angle between the soil and the pile wall; P_0 is the effective overburden pressure.

2.2 USACE Method

The recommended method to determine the outer shaft friction of piles in cohesive soil in USACE is the same as the API method, as shown in Eq. (2). An alternate procedure developed by Semple and Rigden (1984) is adopted to obtain values of α which are especially applicable for very long piles:

$$\alpha = \alpha_1\, \alpha_2 \tag{5}$$

$$\alpha_1 = \begin{cases} 1 & , \quad \dfrac{c_u}{P_o} \le 0.35 \\ 1 - \dfrac{0.5}{0.45}\left(\dfrac{c_u}{P_o} - 0.35\right) & , \quad 0.35 < \dfrac{c_u}{P_o} < 0.8 \\ 0.5 & , \quad \dfrac{c_u}{P_o} \ge 0.8 \end{cases} \tag{6}$$

$$\alpha_2 = \begin{cases} 1 & , \quad \dfrac{L}{D} \le 50 \\ 1 - \dfrac{0.3}{70}\left(\dfrac{L}{D} - 50\right) & , \quad 50 < \dfrac{L}{D} < 120 \\ 0.7 & , \quad \dfrac{L}{D} \ge 120 \end{cases} \tag{7}$$

For design purposes, USACE established that the outer shaft friction of piles in sand increases linearly to an assumed critical depth (z_c) and then remains constant below the critical depth. The

critical depth varies between 10 to 20 D, depending on the relative density of the sand. The guideline for critical depths in sand is included in Table 1.

Table 1 Guidelines for critical depth in sands (USACE 1990)

Sand density	Critical depth (z_c)
Loose	10D
Medium dense	15D
Dense	20D

The unit skin friction acting on the pile shaft may be determined by Eq. (4), where P_0 is evaluated by the following equation:

$$\begin{cases} P_0 = \gamma' z, & z < z_c \\ P_0 = \gamma' z_c, & z \geq z_c \end{cases} \tag{8}$$

2.3 CPH Method

The ultimate shaft friction of driven piles is recommended by the Chinese code (Ministry of Communications of People's Republic of China 2012) according to embedment depth and soil conditions, including void ratio and liquidity index of muddy clay (I_L), plasticity index of clay (I_p), relative density of sand, and standard penetration blow count of medium coarse sand (N). The reference values of ultimate shaft friction for driven piles are provided in Table 2.

2.4 Test Description

In order to investigate the distribution of shaft friction along the depth of large-diameter steel pipe piles, four axial pile load tests were performed on instrumented open-ended piles at two different offshore wind farms (site A and site B) in China. Test piles with different diameters were tested with the anchored pile method more than one month after pile driving. The details of test piles are listed in Table 3.

Offshore Wind Farm A

The tests were conducted on two 62.5 m-long and 60.5 m-long open-ended steel pipe piles with an outer diameter of 2 m and wall thickness of 28 mm. The layout of the test is shown in Fig. 3, S1 and S2 are the test piles, and piles numbering from M1 to M8 are anchorage piles with the batter ratio of 5:1.

Offshore Wind Farm B

The tests were conducted on two 39.9 m-long open-ended steel pipe piles with an outer diameter of 1.8 m and wall thickness of 30 mm. The layout of the test is shown in Fig. 4. S3 and S4 are the test piles, piles numbering from M9 to M14 are anchorage piles, and piles numbering from J1 to J4 are reference piles.

To understand the load-transfer mechanism, two distributed optical fiber sensors were attached to the inside wall of each test pile with a spacing of 0.5 m. Pile deflections were measured at two height levels by linear variable differential transformers that were fixed on the reference beam.

Table 2 Reference values of ultimate shaft friction for driven piles (kPa)

Soil	Soil type	Embedded depth (m)															
		0 ~ 2	2 ~ 4	4 ~ 6	6 ~ 8	8 ~ 10	10 ~ 13	13 ~ 16	16 ~ 19	19 ~ 22	22 ~ 26	26 ~ 30	30 ~ 35	35 ~ 40	40 ~ 45	45 ~ 50	> 50
Muddy clay	$I_L > 1.0$ $1.5 < e \leq 2.4$	2 ~ 4	4 ~ 6	6 ~ 8	8 ~ 10	10 ~ 12	12 ~ 14	14 ~ 16	16 ~ 18	18 ~ 20	18 ~ 20	18 ~ 20	18 ~ 20	18 ~ 20	18 ~ 20	18 ~ 20	18 ~ 20
Clay $I_p > 17$	$I_L > 1.0$	4 ~ 7	6 ~ 9	9 ~ 12	11 ~ 14	13 ~ 16	15 ~ 18	17 ~ 20	18 ~ 21	20 ~ 23	20 ~ 23	20 ~ 23	20 ~ 23	20 ~ 23	20 ~ 23	20 ~ 23	20 ~ 23
	$0.75 < I_L \leq 1.0$	11 ~ 14	14 ~ 17	18 ~ 21	21 ~ 24	23 ~ 26	26 ~ 29	30 ~ 33	33 ~ 36	34 ~ 36	38 ~ 41	43 ~ 46	43 ~ 46	43 ~ 46	43 ~ 46	43 ~ 46	43 ~ 46
	$0.5 < I_L \leq 0.75$	26 ~ 34	30 ~ 38	33 ~ 41	36 ~ 44	40 ~ 48	43 ~ 51	47 ~ 55	51 ~ 59	44 ~ 47	56 ~ 64	58 ~ 66	62 ~ 70	64 ~ 71	64 ~ 71	64 ~ 71	64 ~ 71
	$0.25 < I_L \leq 0.5$	30 ~ 39	34 ~ 43	38 ~ 47	41 ~ 50	45 ~ 54	48 ~ 57	53 ~ 62	57 ~ 66	59 ~ 63	63 ~ 72	65 ~ 74	69 ~ 78	73 ~ 81	73 ~ 81	73 ~ 81	73 ~ 81
	$0 < I_L \leq 0.25$	42 ~ 51	46 ~ 55	50 ~ 59	54 ~ 63	58 ~ 67	61 ~ 70	66 ~ 75	71 ~ 80	75 ~ 84	77 ~ 86	79 ~ 88	84 ~ 93	88 ~ 97	88 ~ 97	88 ~ 97	88 ~ 97
Silty clay $10 < I_p \leq 17$	$I_L > 1.0$	10 ~ 12	13 ~ 15	16 ~ 18	19 ~ 21	21 ~ 23	23 ~ 25	26 ~ 28	28 ~ 30	30 ~ 32	30 ~ 32	30 ~ 32	30 ~ 32	30 ~ 32	30 ~ 32	30 ~ 32	30 ~ 32
	$0.75 < I_L \leq 1.0$	22 ~ 25	25 ~ 28	28 ~ 31	31 ~ 34	33 ~ 36	36 ~ 39	39 ~ 42	41 ~ 44	43 ~ 46	43 ~ 46	43 ~ 46	43 ~ 46	43 ~ 46	43 ~ 46	43 ~ 46	43 ~ 46
	$0.5 < I_L \leq 0.75$	30 ~ 37	34 ~ 41	37 ~ 44	40 ~ 47	43 ~ 50	46 ~ 53	50 ~ 57	54 ~ 61	58 ~ 65	59 ~ 66	61 ~ 68	64 ~ 71	64 ~ 71	64 ~ 71	64 ~ 71	64 ~ 71
	$0.25 < I_L \leq 0.5$	40 ~ 48	44 ~ 52	47 ~ 55	51 ~ 59	54 ~ 62	57 ~ 65	62 ~ 70	66 ~ 74	69 ~ 77	71 ~ 79	73 ~ 81	73 ~ 81	73 ~ 81	73 ~ 81	73 ~ 81	73 ~ 81
	$0 < I_L \leq 0.25$	47 ~ 55	51 ~ 59	55 ~ 63	59 ~ 67	62 ~ 70	66 ~ 74	71 ~ 79	75 ~ 83	79 ~ 87	81 ~ 89	83 ~ 91	88 ~ 96	92 ~ 100	92 ~ 100	92 ~ 100	92 ~ 100
Silt $I_p \leq 10$	$0.75 < I_L \leq 1.0$	21 ~ 27	24 ~ 30	27 ~ 33	30 ~ 36	33 ~ 39	35 ~ 41	39 ~ 45	43 ~ 49	45 ~ 52	45 ~ 53	45 ~ 53	45 ~ 53	45 ~ 53	45 ~ 53	45 ~ 53	45 ~ 53
	$0.5 < I_L \leq 0.75$	25 ~ 33	28 ~ 36	31 ~ 39	34 ~ 42	36 ~ 44	39 ~ 47	41 ~ 49	44 ~ 52	46 ~ 54	46 ~ 54	46 ~ 54	46 ~ 54	46 ~ 54	46 ~ 54	46 ~ 54	46 ~ 54
	$0.25 < I_L \leq 0.5$	34 ~ 42	37 ~ 45	41 ~ 49	44 ~ 52	46 ~ 54	49 ~ 57	52 ~ 60	55 ~ 63	57 ~ 65	58 ~ 66	59 ~ 67	61 ~ 69	61 ~ 69	61 ~ 69	61 ~ 69	61 ~ 69
	$0 < I_L \leq 0.25$	43 ~ 51	47 ~ 55	50 ~ 58	54 ~ 62	57 ~ 65	60 ~ 68	64 ~ 72	68 ~ 76	72 ~ 80	73 ~ 81	75 ~ 83	79 ~ 87	82 ~ 90	85 ~ 93	85 ~ 93	85 ~ 93
Fine sand	Loose	25 ~ 33	28 ~ 36	31 ~ 39	34 ~ 42	36 ~ 44	39 ~ 47	41 ~ 49	44 ~ 52	46 ~ 54	46 ~ 54	46 ~ 54	46 ~ 54	46 ~ 54	46 ~ 54	46 ~ 54	46 ~ 54
	Medium dense	34 ~ 42	37 ~ 45	41 ~ 49	44 ~ 52	46 ~ 54	49 ~ 57	52 ~ 60	55 ~ 63	57 ~ 65	58 ~ 66	59 ~ 67	61 ~ 69	61 ~ 69	61 ~ 69	61 ~ 69	61 ~ 69
	Dense	43 ~ 51	47 ~ 55	50 ~ 58	54 ~ 62	57 ~ 65	60 ~ 68	64 ~ 72	68 ~ 76	72 ~ 80	73 ~ 81	75 ~ 83	79 ~ 87	82 ~ 90	85 ~ 93	85 ~ 93	85 ~ 93
Medium coarse sand	$N > 30$	55 ~ 65	60 ~ 70	64 ~ 74	68 ~ 78	72 ~ 82	76 ~ 86	82 ~ 92	87 ~ 97	92 ~ 102	94 ~ 104	97 ~ 107	103 ~ 113	108 ~ 118	113 ~ 123	118 ~ 128	118 ~ 128

Table 3 Description of test piles

Site	Test piles	Diameter (m)	Thickness (mm)	Embedded depth (m)	Height difference of the inner and outer ground surface (m)	Type	Anchorage piles
A	S1	2.0	28	55	0.5	Steel pipe pile	M1 through M8
	S2	2.0	28	53	0.4	Steel pipe pile	
B	S3	1.8	30	29.3	0.7	Steel pipe pile	M9 through M14
	S4	1.8	30	29.3	0.7	Steel pipe pile	

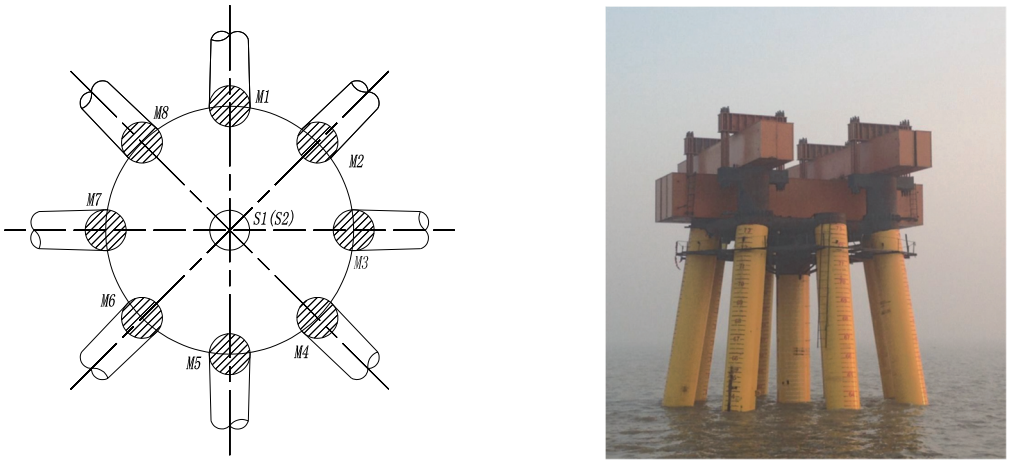

(a) Layout chart (b) Reaction frame loading system

Fig. 3 Layout chart and reaction frame loading system of S1 and S2

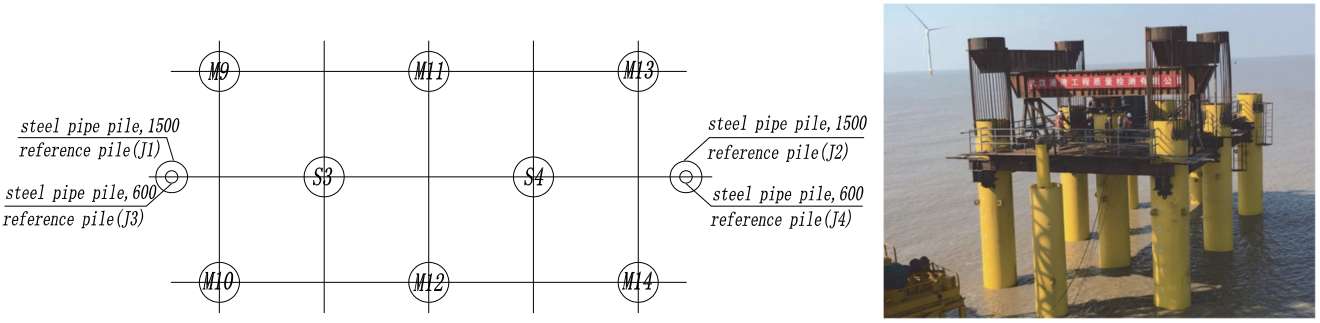

(a) Layout chart (mm) (b) Test platform

Fig. 4 The layout chart and test platform of S3 and S4

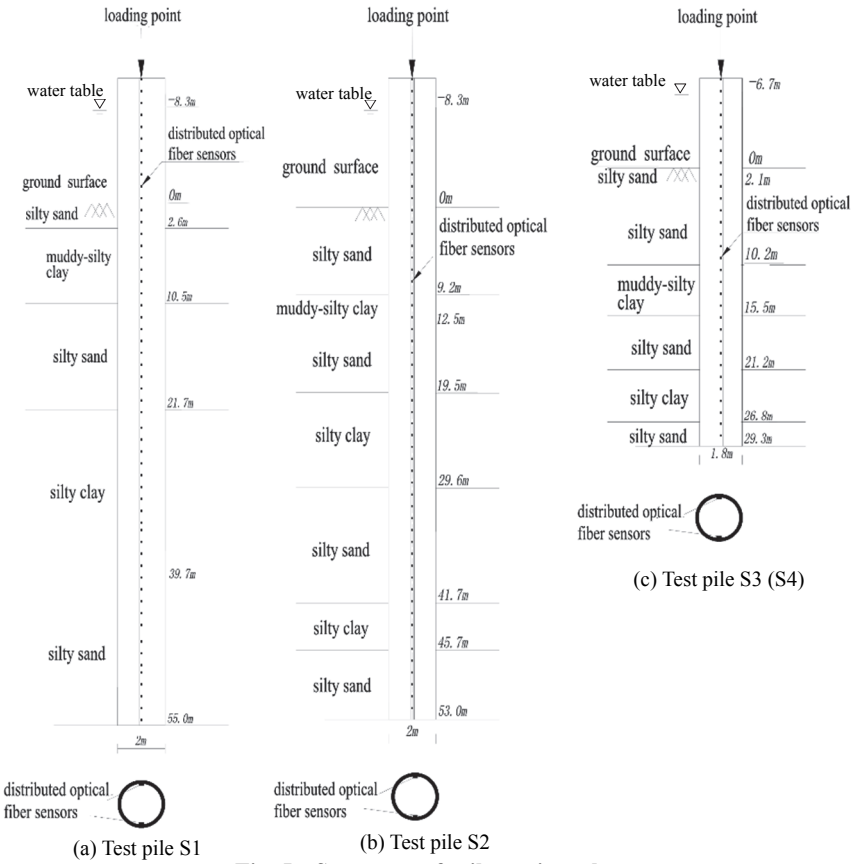

(a) Test pile S1 (b) Test pile S2 (c) Test pile S3 (S4)

Fig. 5 Summary of soil stratigraphy

Table 4 Soil layer distributions and mechanical properties of subsoil (Site A)

Soil	Total unit weight (kN/m^3)	Undrained shear strength (kPa)	Internal friction angle (°)	Plasticity index (%)	Modulus of compressibility (MPa)
Silty sand	19.1	–	30	–	6.8
Muddy-silty clay	17.4	19.8	–	15.6	3.1
Silty sand	19.8	–	32	–	13.9
Silty clay	18.1	30	–	15.9	4.4
Silty sand	20.2	–	33	–	17.4

Table 5 Soil layer distributions and mechanical properties of subsoil (Site B)

Soil	Total unit weight (kN/m^3)	Undrained shear strength (kPa)	Internal friction angle (°)	Plasticity index (%)	Modulus of compressibility (MPa)
Silty sand	19.5	–	28	–	4.5
Silty sand	19.7	–	30	–	5.4
Muddy-silty clay	18.1	20	–	15.2	3.5
Silty sand	19.8	–	32	–	8.6
Silty clay	18.7	30	–	16.4	4.5
Silty sand	19.7	–	34	–	11.5

The subsurface investigation was performed at three boreholes nearby the test piles. In order to evaluate the properties of subgrade in which the piles were installed, soil classification tests, triaxial tests, consolidation tests, and unconfined compression tests were performed. Figure 5 shows the subsurface profile nearby the test piles. The properties of subsoils of two sites are listed in Table 4 and Table 5.

3. FIELD TEST DATA ANALYSIS

According to the Specification for Testing of Pile Under Static Load in Harbor Engineering (Ministry of Communications of People's Republic of China 2002), load can be terminated if one of the following conditions is met: 1) the total settlement of the pile exceeds 40 mm, and the load-settlement curve descends sharply; 2) the settlement is unstable within 24 hours. The slow sustaining load method was applied in the axial loading tests. The load was applied by stages, and the load increment was 4,100 kN for S1 (S2) and 2,300 kN for S3 (S4). The load-settlement curves for the test piles are depicted in Fig. 6.

The test results show that the ultimate bearing capacities for S1 and S2 are 32,800 kN and 34,850 kN, and the corresponding settlements are 50.43 mm and 58.73 mm, respectively. The pile top settlements under the maximum load are 106.51 mm and 106.44 mm, and the residual settlements after unloading are 68.09 mm and 64.26 mm, respectively. For S3 and S4, the ultimate bearing capacities are 12,650 kN and 13,800 kN, and the corresponding settlements are 33.81 mm and 47.17 mm, respectively. The pile top settlements under the maximum load are 73.47 mm and 73.03 mm, and the residual settlements after unloading are 69.11 mm and 61.15 mm, respectively.

Figure 7 shows the axial force profile along the depth. In the figure, the curve exhibits an inflection point nearby the ground surface, indicating that the shaft friction begins to take effect in this location. The axial force approximately linearly decreases along the depth. The shaft resistance reached a limit value before the final load step, while the tip resistance was still increasing at the final load step. Thus, the limit shaft resistance was determined as that mobilized at the final load step.

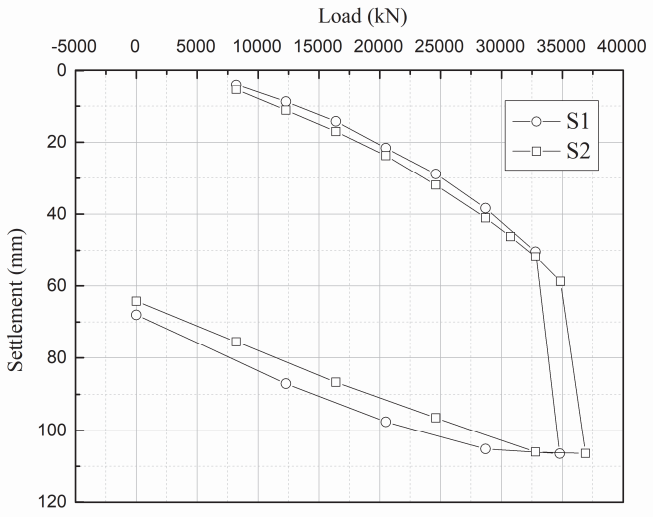

(a) S1 and S2

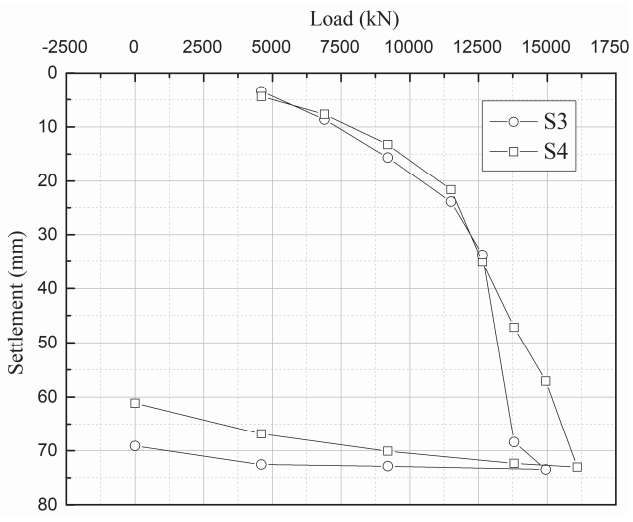

(b) S3 and S4

Fig. 6 Load-settlement curves of test piles

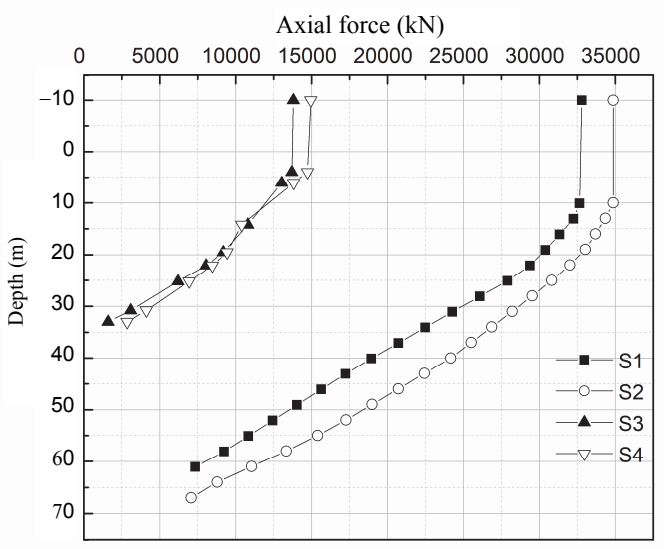

Fig. 7 Derived profiles of axial force

The outer shaft friction of section i were calculated by API method, USACE method, and CPH method, whereas the inner shaft friction of section i were calculated by Eq. (1). Then, the distribution curves for inner and outer friction-resistance ratio for each pile were depicted in Fig. 8.

In Figure 8, the inner and outer friction-resistance ratio increases with depth. For the API method and USACE method, the range is rather small in comparison to the CPH method. The values of f_{ins}/f_{out} at different depths are shown in Table 6, and the following observations are made:

(a) The ratio of f_{ins}/f_{out} at the upper 3 m of the embedded part of the pile varies from 0.03 to 0.25 (0.12 on average) for cohesive soil and varies from 0.08 to 0.27 (0.16 on average) for cohesionless soil. This indicates that the inner shaft friction close to ground surface is indispensable.

(b) A trend of an increasing portion of the inner shaft friction to the outer shaft friction with depth is visible. At the critical depth region, the average ratio of f_{ins}/f_{out} varies from 0.28 to 0.43 for cohesive soil and varies from 0.26 to 0.40 for cohesionless soil.

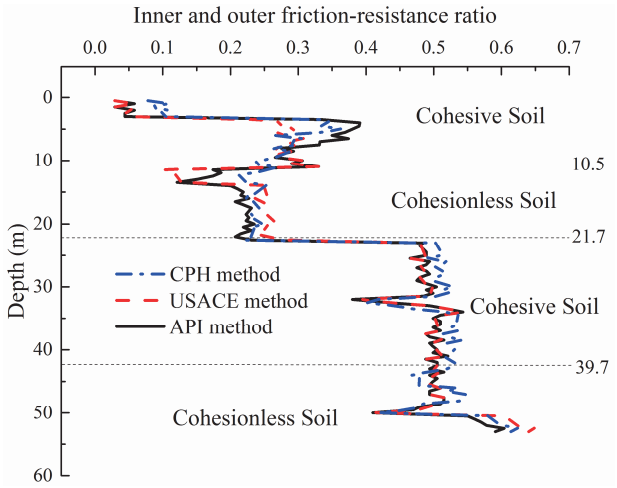

(a) S1

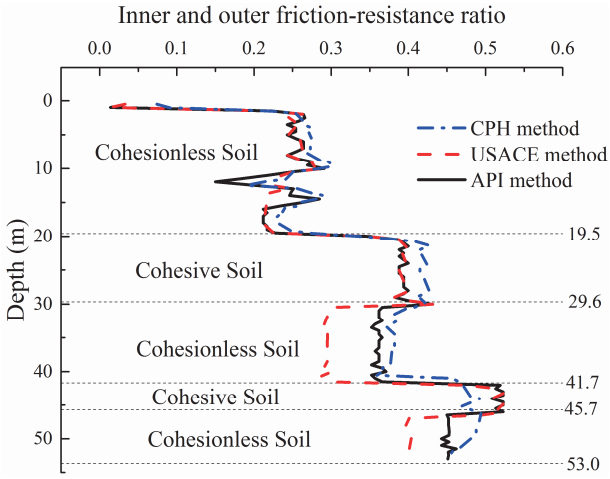

(b) S2

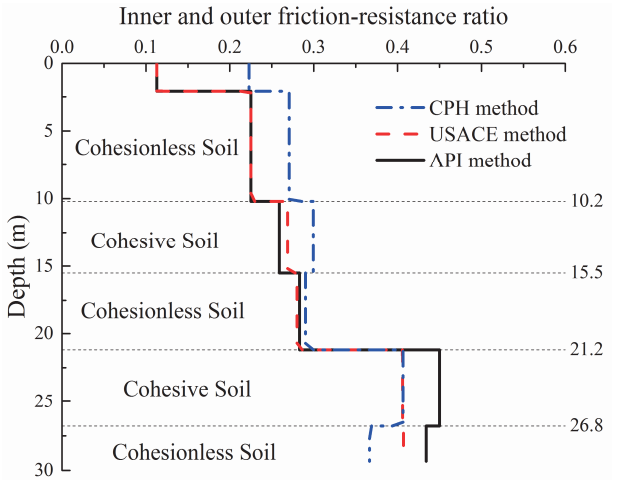

(c) S3

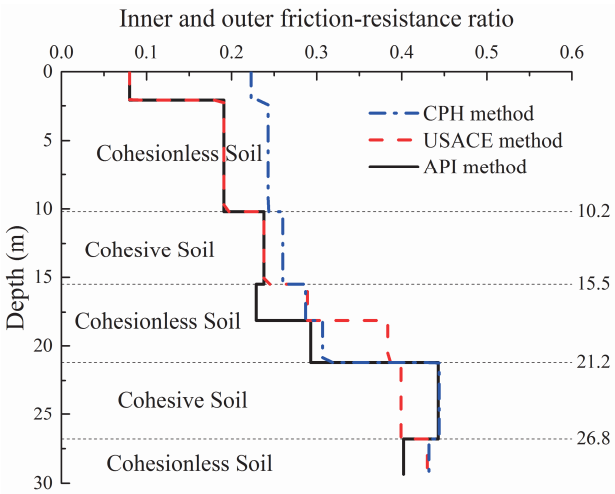

(d) S4

Fig. 8 Derived profiles of inner and outer friction-resistance ratio

Table 6 Values of f_{ins}/f_{out} at different depths

Depth (m)	Cohesive soil		Cohesionless soil	
	Range value	Average	Range value	Average
0 ~ 3	0.03 ~ 0.25	0.12	0.08 ~ 0.27	0.16
3 ~ 10	0.25 ~ 0.36	0.28	0.25 ~ 0.30	0.26
10 ~ 20	0.25 ~ 0.40	0.30	0.23 ~ 0.38	0.28
20 ~ 30	0.47 ~ 0.54	0.43	0.36 ~ 0.43	0.40
30 ~ 40	0.46 ~ 0.55	0.50	0.36 ~ 0.52	0.46
> 40	–	–	0.40 ~ 0.65	0.50

(c) Furthermore, the inner and outer friction-resistance ratio continues to increase as it goes deeper, and the maximum ratio is no more than 0.5.

4. PROPOSED DESIGN METHOD

Based on the field axial loading test results and the previous analysis results, the following equations are introduced to predict the inner and outer friction-resistance ratio.

Cohesive Soil:

$$f_{ins}/f_{out} = a + b\psi + c\psi^2 \tag{9}$$

where $\psi = P_0/c_u$; P_0 is the effective overburden pressure; c_u is the undrained shear strength of soil; a, b, and c are fitting coefficients.

Cohesionless Soil:

$$f_{ins}/f_{out} = d + e\xi' \tag{10}$$

where $\xi' = \dfrac{z}{D\tan\varphi}$, φ is the internal friction angle of the soil; z is the embedded depth; d and e are fitting coefficients.

The ratios of f_{ins}/f_{out} at different depths were fitted according to the test data, and the results are given in Table 7.

Table 7 Recommendation values of fitting coefficients

Depth (m)	Cohesive soil			Cohesionless soil	
	a	b	c	d	e
0 ~ 3	0.039	0.071	– 0.048	0.112	0.030
3 ~ 10	0.388	– 0.118	0.029	0.158	0.006
10 ~ 20	0.022	0.057	– 0.001	0.081	0.011
20 ~ 30	0.850	– 0.265	0.038	– 0.062	0.018
30 ~ 40	0.000	0.175	– 0.015	0.449	– 0.004
> 40	0.737	– 0.080	0.006	0.122	0.009
Average	0.339	– 0.027	0.002	0.143	0.012

To validate the proposed model, the inner and outer friction-resistance ratios predicted by Eqs. (9) and (10) are compared with the results calculated by the API, USACE and CPH methods. Here, the outer shaft friction is averaged by the previous three methods. The comparison results are shown in Fig. 9.

The comparison shows that the average values of f_{ins}/f_{out} calculated by the three methods and this study are very close for S2. In the depth range of 10 ~ 30 m of S1, the predictions by this study are smaller than the calculated values, whereas in the depth range of 10 ~ 20 m of S3 and S4, the results show the opposite trend, and the prediction accuracy is acceptable.

For large diameter open-ended steel pipe piles, the pile bearing capacity is composed of annulus, inner and outer shaft resistances. In order to separate all the resistances components, the instrumented double-walled pile system (Lehane and Gavin 2001; Paik and Salgado 2003) can be used. This technique has been applied to many laboratory model pile tests but had never been used in full-scale field tests. The new design method proposed in this paper assuming that the outer shaft friction given by three different empirical analytical methods, and the total shaft resistances (the sum of inner and outer shaft resistances) of section i is investigated by strain gauges, then the inner shaft resistance and f_{ins}/f_{out} of different sections can be obtained. Due to the limit of conditions, this technique is also not used in this paper. To validate and improve the efficiency of the proposed design method, a focus will be put on the instrumented double-walled pile system to separate the inner and outer shaft resistances in future research.

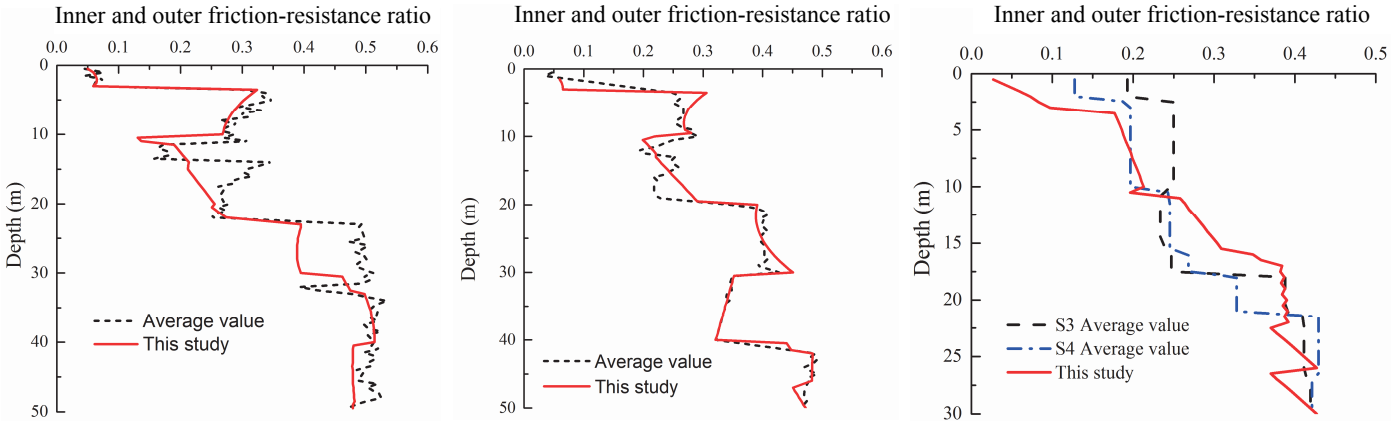

(a) S1 (b) S2 (c) S3 and S4

Fig. 9 Comparison results of test piles

5. CONCLUSIONS

A series of full-scale axial load tests of open-ended steel pipe piles are conducted at two thick overburden-layer sites. By assuming that the outer shaft friction given by the API, USACE and CPH methods is suitable for these sites, the inner and outer friction-resistance ratio along the pile shaft are derived. An effort has been made to develop a new design method to correlate the inner shaft resistance to the axial bearing capacity. The main conclusions are as follows:

1. The inner shaft friction is indispensable for large-diameter open-ended steel pipe piles, and the piles are approximately full cored. At the upper 3 m close to the ground surface, the inner and outer friction-resistance ratio is relatively small, and the average value is about 0.15. A trend of an increasing portion of the inner shaft friction to the outer shaft friction with depth is visible. At the critical depth region, the average ratio varies from 0.28 to 0.43 for cohesive soil and varies from 0.26 to 0.40 for cohesionless soil. Futhermore, the ratio continues to increase as it goes deeper, and the maximum ratio is no more than 0.5.
2. The case studies on offshore large-diameter pipe piles in thick overburden-layer show the importance of pile diameter and embedded depth to the capactiy design. Comparison with the field tests shows that the prediction results of the new design method are in good agreement to the measured inner and outer friction-resistance ratio. The results of this study can serve as a guide to help engineers to advance the understanding of the axial load response behavior of an offshore foundation.

FUNDING

The authors were supported financially by the National Natural Science Foundation of China (Grant No. U1865201) and the Foundation of PowerChina Chengdu Engineering Corporation Limited (Grant No. P43919).

DATA AVAILABILITY

The data and/or computer codes used/generated in this study are available from the corresponding author on reasonable request.

REFERENCES

American Petroleum Institute (API). (2010). *Recommended Practice for Planning, Designing and Constructing Fixed Offshore Platforms-Working Stress Design*. Washington, D.C: American Petroleum Institute Publishing Services.

Clausen, C.J.F., Aas, P.M., and Karlsrud, K. (2005). "Bearing capacity of driven piles in sand, the NGI approach." *ISFOG 2005-Proceedings of the 1st International Symposium on Frontiers in Offshore Geotechnics*, Perth, 677-682.

Jardine, R., Chow, F., and Overy, R. *et al.* (2005). *ICP Design Methods for Driven Piles in Sands and Clays*. Thomas Telford Publishing, London, 1-14.

Kolk, H.J., Baaijens, A.E., and Senders, M. (2005). "Design criteria for pipe piles in silica sands." *ISFOG 2005-Proceedings of the 1st International Symposium on Frontiers in Offshore Geotechnics*, Perth, 711-716.

Kyuho, P., Rodrigo, S., and Junhwan, L. *et al.* (2003). "Behavior of open and closed-ended piles driven into sands." *Journal of Geotechnical and Geoenvironmental Engineering*, ASCE, **129**(4), 296-306. http://doi.org/10.1061/(ASCE)1090-0241(2003)129:4(296)

Lehane, B.M. and Gavin, K.G. (2001). "Base resistance of jacked pipe piles in sand." *Journal of Geotechnical and Geoenvironmental Engineering*, ASCE, **127**(6), 473-480. http://doi.org/10.1061/(asce)1090-0241(2001)127:6(473)

Lehane, B.M., Schneider, J.A., and Xu, X. (2005). "The UWA-05 method for prediction of axial capacity of driven piles in sand." *ISFOG 2005-Proceedings of the 1st International Symposium on Frontiers in Offshore Geotechnics*, Perth, 683-690.

Lüking, J. and Becker, P. (2015). "Harmonisierung der Berechnungsverfahren der axialen Tragfähig-keit für offene Profile nach EA-Pfähle und EAU." *Bautechnik*, **92**(2), 161-176. http://doi.org/10.1002/bate.201400062

Ministry of Communications of People's Republic of China. (2002). *Specification for Testing of Pile Under Static Load in Harbor Engineering*. Beijing: China Communications Press.

Ministry of Communications of People's Republic of China. (2012). *Code for Pile Foundation of Harbor Engineering*. Beijing: China Communications Press.

Paik, K.H. and Salgado, R. (2003). "Determination of the bearing capacity of open-ended piles in sand." *Journal of Geotechnical and Geoenvironmental Engineering*, ASCE, **129**(1), 46-57. http://doi.org/10.1061/(ASCE)1090-0241(2003)129:1(46)

Paikowsky, S.G. and Whitman, R.V. (1990). "The effects of plugging on pile performance and design." *Canadian Geotechnical Journal*, **27**(4), 429-440. http://doi.org/10.1139/t90-059

Semple, R.M. and Rigden, W.J. (1984). "Shaft capacity of driven pipe piles in clay." *Ground Engineering*, **19**(1), 11-19.

USACE (1990). *Engineering and Design-Settlement Analysis*. U.S. Army Corps of Engineers, Engineer Manual. 1110-1-1904.

Yu, F. and Yang, J. (2012). "Base capacity of open-ended steel pipe piles in sand." *Journal of Geotechnical and Geoenvironmental Engineering*, ASCE, **138**(9), 1116-1128. http://doi.org/10.1061/(ASCE)GT.1943-5606.0000667

Yu, F. and Yang, J. (2012). "Improved evaluation of interface friction on steel pipe pile in sand." *Journal of Performance of Constructed Facilities*, **26**(2), 170-179. http://doi.org/10.1061/(ASCE)CF.1943-5509.0000256